JOURNAL OF GUIDANCE, CONTROL, AND DYNAMICS
Vol. 34, No. 3, May–June 2011

Explicit Frequency-Shaped Coning Algorithms for Pseudoconing Environments

Paul G. Savage*
Strapdown Associates, Inc., Maple Plain, Minnesota 55359

DOI: 10.2514/1.51600

Explicit Frequency Shaping is a numerical coning algorithm design process based on least-squares minimization of algorithm error over an expected coning environment frequency range. In its original published form, the Explicit method was formulated based on error-free gyro data. This paper extends the Explicit concept to include compensation of coninglike dynamic errors (pseudoconing) present on the algorithm inputs. Examples are provided for cases where pseudoconing is an analytically definable function of gyro dynamic response and when it is an ill-defined high-frequency presence that may potentially exist on gyro outputs. Numerical results are presented comparing the new Extended Explicit technique with previous Explicit and Taylor frequency-series expansion-based coning algorithm design approaches.

Introduction

MODERN strapdown inertial navigation system (INS) computation algorithms apply a coning correction to sensed gyro outputs in the attitude updating process. The analytical basis for many coning correction algorithms is optimum performance in a pure coning environment as originated by Miller in 1983 [1] and refined by Ignagni in 1990 and 1996 [2,3]. Algorithm coefficients were based on a truncated Taylor series expansion of the desired algorithm response in powers of coning frequency. Each of the aforementioned approaches were based on operation with error-free gyro inputs.

The coning correction design methodology used in [1] differs from that of [2,3]. In [2,3], the coning correction was derived for a pure unconstrained coning environment as an approximation to the integrated coning portion of the Laning rotation vector rate equation [4] over an attitude update cycle. The coning portion is that part of the rotation vector rate generated by rotation of the strapdown gyro sensed angular rate vector (the analytical definition of coning motion). In the absence of coning motion, a body will rotate around the angular rate vector with the rate vector components maintaining a constant angular orientation in both body fixed and nonrotating inertial axes. An unconstrained pure coning environment is defined as the condition where two orthogonal axes in a rotating body experience sinusoidal angular rate oscillations that are mutually phase shifted by 90 deg. Under this condition, the angular motion of the third body axis will trace a conical surface in inertial space (coning motion) with cone half angle equal to the integrated angular rate input amplitude, and with frequency around the cone (coning frequency) equal to the input rates oscillation frequency. Simultaneously, the angular rate vector will rotate in body axes at the angular rate oscillation frequency, and the body will develop a constant inertial attitude rate component (coning rate) about the cone axis with magnitude per angular rate oscillation cycle equal to π times the square of the integrated angular rate magnitude.

In contrast with the [2,3] unconstrained-coning-motion/integrated-rotation-vector-coning-rate approach, the coning correction in [1] was designed for constrained pure coning motion as the body axis rotation vector producing attitude change minus the corresponding integrated gyro sensed angular rate. A constrained pure coning environment is defined as the condition where the average total rotation rate of a body in inertial space is constrained to zero while two orthogonal axes fixed in the body are experiencing sinusoidal angular rate oscillations that are mutually phase shifted by 90 deg. Constrained coning motion is created by simultaneously applying a constant angular rate about the third body axis equal to the negative of the previously defined coning rate. Coning correction algorithm coefficients designed using the [1] approach are identical to those of [2,3] for error-free gyro inputs.

In 2001, Mark and Tazartes [5] extended the [1] frequency-series design approach for constrained coning motion to include compensation for coninglike dynamic errors on the angular rate input to the attitude updating process caused by dynamic shaping on the strapdown gyro data. This was achieved based on a hypothesized constrained coning environment for which the oscillatory rate components were the actual sensed orthogonal angular rate inputs (i.e., including the gyro dynamic shaping transfer function gain at the oscillation frequency). As in [1], the coning correction was designed as the body axis rotation vector producing attitude change minus the corresponding integrated gyro sensed angular rate. Unlike [1], however, attitude change was defined to be the hypothesized (not the actual) constrained coning motion with corresponding integrated gyro sensed angular rate defined as the actual measured gyro output rate (but using unity for the dynamic transfer function gain on the constant third gyro output as would be generated under actual constrained coning). The coning correction algorithm would then create a constrained coning motion solution in a strapdown system computer when using gyro data containing dynamic error under actual constrained coning motion.

In 2010, the author introduced an Explicit Frequency Shaping concept for coning correction algorithm design [6] based on minimizing algorithm error in a least-squares sense over a user specified coning frequency range. As in [2,3], the [6] approach was based on error-free gyro inputs in an unconstrained coning environment. This paper describes an extended version of the [6] approach designed to accommodate gyro inputs containing general coninglike errors (pseudoconing). As in [2,3,6], the extended Explicit approach is for optimization in an unconstrained coning environment. In this case, however, optimization is based on generating a true solution for the total inertial attitude change over an attitude update cycle. References [2,3,6] were based on achieving a true solution for the integrated coning portion of the body axis rotation vector rate over the attitude update cycle. As will be shown subsequently, the latter approach is not applicable to gyro inputs containing pseudoconing whereas the former applies to inputs that may or may not contain pseudoconing.

Received 15 July 2010; revision received 10 Aug. 2010; accepted for publication 10 Aug. 2010.

*President; pgs@strapdownassociates.com. Senior Member AIAA.

Design Approach for the Extended Explicit Coning Algorithm

In a strapdown INS, the angular orientation (attitude) of the inertial sensor assembly is typically represented as a direction cosine matrix or quaternion, computed as an integration process from gyro sensed angular rate data. For a direction cosine implementation, the attitude rate of change is given by the following well-known differential equation ([2] and [7] Sec. 3.3.2):

$$\dot{C} = C(\underline{\omega}\times) \tag{1}$$

where C is a direction cosine matrix representing attitude relative to a reference coordinate space (e.g., inertial nonrotating), $\underline{\omega}$ is the strapdown gyro sensed angular rate vector, and for an arbitrary vector $\underline{V}$, the skew symmetric operator $(\underline{V}\times)$ is

$$\begin{bmatrix} 0 & -V_z & V_y \\ V_z & 0 & -V_x \\ -V_y & V_x & 0 \end{bmatrix}$$

composed of $\underline{V}$ components.

For attitude updated at an l cycle computation rate, the integral of Eq. (1) at each l cycle can be represented as

$$\Delta C(t) = \int_{t_{l-1}}^{t} [C_{l-1} + \Delta C(\tau)](\underline{\omega}\times)\,\mathrm{d}\tau = C_{l-1}(\underline{\alpha}(t)\times) + \int_{t_{l-1}}^{t} \Delta C(\tau)(\underline{\omega}\times)\,\mathrm{d}\tau$$

$$\underline{\alpha}(t) \equiv \int_{t_{l-1}}^{t} \underline{\omega}\,\mathrm{d}\tau \qquad \Delta C_l \equiv \Delta C(t_l) \qquad C_l = C_{l-1} + \Delta C_l \tag{2}$$

The analytically equivalent algorithmic version of the total attitude change ΔC_l in Eq. (2) is the well-known form ([6] and [7] Sec. 7.1.1.1)

$$\Delta C_l = C_{l-1}[f_1(\phi_l)(\underline{\phi}_l\times) + f_2(\phi_l)(\underline{\phi}_l\times)^2]$$

$$f_1(\phi_l) = \frac{\sin\phi_l}{\phi_l} = \sum_{i=1}(-1)^{i-1}\frac{\phi_l^{2(i-1)}}{(2i-1)!}$$

$$f_2(\phi_l) = \frac{1}{\phi_l^2}(1-\cos\phi_l) = \sum_{i=1}(-1)^{i-1}\frac{\phi_l^{2(i-1)}}{(2i)!}$$

$$\underline{\phi}_l = \underline{\alpha}_l + \delta\underline{\phi}_l \qquad \delta\underline{\phi}_l \approx \int_{t_{l-1}}^{t_l}\frac{1}{2}\underline{\alpha}(t)\times\underline{\omega}\,\mathrm{d}t$$

$$\underline{\alpha}(t) = \int_{t_{l-1}}^{t}\underline{\omega}\,\mathrm{d}\tau \qquad \underline{\alpha}_l = \underline{\alpha}(t_l) \tag{3}$$

where $\underline{\phi}_l$ is a rotation vector representing the change in sensor assembly attitude (in body axes) over an l cycle and $\delta\underline{\phi}_l$ (computed as an approximation to the integrated coning portion of the [4] rotation vector rate equation) has been denoted as the coning correction to the integrated gyro sensed angular rate increment $\underline{\alpha}_l$. For a quaternion formulation, $\underline{\phi}_l$ is used similarly to update the quaternion. [Note: [2,3,6,8] and [7] Sec. 7.1.1.1, show how the coning correction $\delta\underline{\phi}_l$ in Eq. (3) can be calculated at the l rate and then used, with no loss in accuracy, to update attitude at slower than the l rate through a two-speed computation structure.]

Now consider a general unconstrained-coning-motion situation having axis a and b angular rate oscillations:

$$\underline{\omega} = \underline{u}_a\theta_{0_a}\Omega\cos\Omega t + \underline{u}_b\theta_{0_b}\Omega\sin\Omega t \tag{4}$$

where $\underline{u}_a$ and $\underline{u}_b$ are mutually orthogonal body fixed unit vectors, and θ_{0_a}, θ_{0_b} are oscillation angular amplitudes about axes $\underline{u}_a$, $\underline{u}_b$. The $\delta\underline{\phi}_l$ term in Eq. (3) accounts for the Eq. (4) type coning motion in the C matrix updating process as a correction to $\underline{\alpha}_l$ gyro data along body fixed axis $\underline{u}_c$ orthogonal to axes $\underline{u}_a$ and $\underline{u}_b$. The object of this paper is to design an algorithm for $\delta\underline{\phi}_l$ that accurately accounts for true coning motion in the attitude updating process, but using Eq. (4) gyro data containing coninglike dynamic errors (pseudoconing).

The [2,3,6] coning correction algorithm design approach was to generate a true value for $\delta\underline{\phi}_l$ in the presence of Eq. (4) coning motion and error-free gyro data. For gyro data containing pseudoconing error, the fallacy in this approach is that it neglects to correct for $\underline{u}_a$ and $\underline{u}_b$ axis dynamic error in the $\underline{\alpha}_l$ portion of $\underline{\phi}_l$ which then multiplies C_{l-1} in Eqs. (3). Because C_{l-1} also contains $\underline{u}_a$ and $\underline{u}_b$ axis dynamic error (from previous ΔC_l summing), its product with the $\underline{\alpha}_l$ errors generates additional $\underline{u}_c$ axis pseudoconing. To also compensate for C_{l-1} $\underline{\alpha}_l$ product error, the coning correction must be designed to generate a true value for the total attitude change in inertial space [e.g., ΔC_l in Eqs. (3)] as described next.

Analytical Basis for the Extended Coning Algorithm

For the following analysis purposes, total attitude C will be represented as a rotation vector $\underline{\Psi}$. For small magnitude angular motion, the rate of change of $\underline{\Psi}$ [analogous to Eq. (1)] can be represented by the following approximate form of the [4] rotation vector rate equation:

$$\dot{\underline{\Psi}}(t) \approx \underline{\omega} + \frac{1}{2}\underline{\psi}(t)\times\underline{\omega} \approx \underline{\omega} + \frac{1}{2}\underline{A}(t)\times\underline{\omega} \qquad \underline{A}(t) \equiv \int_0^t \underline{\omega}\,\mathrm{d}\tau \tag{5}$$

For attitude updated at the l cycle computation rate, the integral of $\dot{\underline{\Psi}}(t)$ in Eq. (5) at the l cycle update times is

$$\Delta\underline{\Psi}(t) = \int_{t_{l-1}}^{t}\left[\underline{\omega} + \frac{1}{2}\underline{A}(\tau)\times\underline{\omega}\right]\mathrm{d}\tau = \underline{\alpha}(t) + \int_{t_{l-1}}^{t}\frac{1}{2}\underline{A}(\tau)\times\underline{\omega}\,\mathrm{d}\tau$$

$$\underline{A}(t) \equiv \int_0^t \underline{\omega}\,\mathrm{d}\tau \qquad \underline{\alpha}(t) \equiv \int_{t_{l-1}}^{t}\underline{\omega}\,\mathrm{d}\tau$$

$$\Delta\underline{\Psi}_l = \Delta\underline{\Psi}(t_l) \qquad \underline{\Psi}_l = \underline{\Psi}_{l-1} + \Delta\underline{\Psi}_l \tag{6}$$

Under Eq. (4) angular rate, it is easily shown analytically from Eq. (6) that the attitude change $\Delta\underline{\Psi}_l$ is given by

$$\Delta\underline{\Psi}_l = \underline{u}_a\theta_{0_a}(\sin\Omega t_l - \sin\Omega t_{l-1}) - \underline{u}_b\theta_{0_b}(\cos\Omega t_l - \cos\Omega t_{l-1}) + \underline{u}_c\dot{\Phi}(\Omega)\left(1 - \frac{\sin\Omega t_l - \sin\Omega t_{l-1}}{\Omega T_l}\right)T_l \tag{7}$$

with

$$\dot{\Phi}(\Omega) \equiv \frac{1}{2}\Omega\theta_{0_a}\theta_{0_b} \tag{8}$$

where $\dot{\Phi}(\Omega)$ is the coning rate. As should be apparent from Eq. (7), $\dot{\Phi}(\Omega)$ represents the average total attitude rotation rate induced about the $\underline{u}_c$ axis due to the Eq. (4) oscillatory angular rate components about axes $\underline{u}_a$ and $\underline{u}_b$.

Using the algorithmic structure in Eq. (3) as a guide, the analytically equivalent form of $\Delta\underline{\Psi}_l$ is from Eq. (6):

$$\Delta\underline{\Psi}_l = \frac{1}{2}\underline{A}_{l-1}\times\underline{\alpha}_l + \underline{\phi}_l \qquad \underline{A}_{l-1} = \sum_{i=1}^{l-1}\underline{\alpha}_i$$

$$\underline{\alpha}(t) = \int_{t_{l-1}}^{t}\underline{\omega}\,\mathrm{d}\tau \qquad \underline{\alpha}_l = \underline{\alpha}(t_l)$$

$$\underline{\phi}_l = \underline{\alpha}_l + \delta\underline{\phi}_l \qquad \delta\underline{\phi}_l = \int_{t_{l-1}}^{t_l}\frac{1}{2}\underline{\alpha}(t)\times\underline{\omega}\,\mathrm{d}t \tag{9}$$

Under Eq. (4) motion, it is readily shown from Eq. (9) that

$$\underline{\alpha}_l = \underline{u}_a\theta_{0_a}(\sin\Omega t_l - \sin\Omega t_{l-1}) - \underline{u}_b\theta_{0_b}(\cos\Omega t_l - \cos\Omega t_{l-1})$$

$$\underline{A}_{l-1} = \underline{u}_a\theta_{0_a}\sin\Omega t_{l-1} + \underline{u}_b\theta_{0_b}(1-\cos\Omega t_{l-1})$$

which when substituted in Eq. (9) finds for the algorithmic form

$$\Delta\underline{\Psi}_l = \underline{u}_a\theta_{0_a}(\sin\Omega t_l - \sin\Omega t_{l-1}) - \underline{u}_b\theta_{0_b}(\cos\Omega t_l - \cos\Omega t_{l-1}) + \underline{u}_c\dot{\Phi}(\Omega)\left(\frac{\sin\Omega T_l}{\Omega T_l} - \frac{\sin\Omega t_l - \sin\Omega t_{l-1}}{\Omega T_l}\right)T_l + \delta\underline{\phi}_l \quad (10)$$

We identify Eq. (10) as the solution generated in the system computer using real gyro data (including errors) and Eq. (7) as representing a true solution based on error-free gyro inputs. For clarity we adopt the following distinguishing notation for Eqs. (7) and (10) with (4) and (8):

$$\Delta\underline{\Psi}_{\mathrm{True}_l} = \underline{u}_a\theta_{0\mathrm{True}_a}(\sin\Omega t_l - \sin\Omega t_{l-1}) - \underline{u}_b\theta_{0\mathrm{True}_b}(\cos\Omega t_l - \cos\Omega t_{l-1}) + \underline{u}_c\dot{\Phi}_{\mathrm{True}}(\Omega)\left(1 - \frac{\sin\Omega t_l - \sin\Omega t_{l-1}}{\Omega T_l}\right)T_l \quad (11)$$

with

$$\underline{\omega}_{\mathrm{True}} = \underline{u}_a\theta_{0\mathrm{True}_a}\Omega\cos\Omega t + \underline{u}_b\theta_{0\mathrm{True}_b}\Omega\sin\Omega t$$
$$\dot{\Phi}_{\mathrm{True}}(\Omega) \equiv \frac{1}{2}\Omega\theta_{0\mathrm{True}_a}\theta_{0\mathrm{True}_b} \quad (12)$$

and

$$\Delta\underline{\Psi}_{\mathrm{Gyro}_l} = \underline{u}_a\theta_{0\mathrm{Gyro}_a}(\sin\Omega t_l - \sin\Omega t_{l-1}) - \underline{u}_b\theta_{0\mathrm{Gyro}_b}(\cos\Omega t_l - \cos\Omega t_{l-1}) + \underline{u}_c\dot{\Phi}_{\mathrm{Gyro}}(\Omega)\left(\frac{\sin\Omega T_l}{\Omega T_l} - \frac{\sin\Omega t_l - \sin\Omega t_{l-1}}{\Omega T_l}\right)T_l + \delta\underline{\phi}_{\mathrm{Gyro}_l} \quad (13)$$

with

$$\underline{\omega}_{\mathrm{Gyro}} = \underline{u}_a\theta_{0\mathrm{Gyro}_a}\Omega\cos\Omega t + \underline{u}_b\theta_{0\mathrm{Gyro}_b}\Omega\sin\Omega t$$
$$\dot{\Phi}_{\mathrm{Gyro}}(\Omega) \equiv \frac{1}{2}\Omega\theta_{0\mathrm{Gyro}_a}\theta_{0\mathrm{Gyro}_b} \quad (14)$$

where True and Gyro designate computational forms using idealized error-free inputs (True), and those using real gyro inputs (Gyro) containing pseudoconing dynamic errors.

For future use we will also write

$$\dot{\Phi}_{\mathrm{Gyro}}(\Omega) = \dot{\Phi}_{\mathrm{True}}(\Omega) + \dot{\Phi}_{\mathrm{Pseudo}}(\Omega) \quad (15)$$

where $\dot{\Phi}_{\mathrm{Pseudo}}(\Omega)$, the pseudoconing error in the Eqs. (14) $\dot{\Phi}_{\mathrm{Gyro}}(\Omega)$ coning rate, is defined in general as caused by gyro errors having the same frequency/phase characteristics as the Eqs. (12) true angular rate $\underline{\omega}_{\mathrm{True}}$, but containing erroneous elements. Note from the form of $\dot{\Phi}_{\mathrm{Gyro}}(\Omega)$ in Eq. (14) that pseudoconing can be caused by combined $\underline{u}_a$ and $\underline{u}_b$ axis erroneous angular rate components, or by a $\underline{u}_a$ or $\underline{u}_b$ axis error coupled with true angular rate component in the other axis at the same frequency (with 90 deg phase shift). It is to be noted that this pseudoconing definition is broader than sometimes used whereby it has been identified as high-frequency coning error created by imperfections in the gyro and sensor assembly mechanical design (e.g., structural resonances excited by external vibrations [5] or by functional internal vibrating elements in some modern day gyro implementations, e.g., mechanical dither in laser gyros [9]), rather than analytically definable dynamic response characteristics inherent in the gyro mechanization or from intentionally added filtering to gyro outputs [5]. To distinguish between the two pseudoconing effects we define

$$\dot{\Phi}_{\mathrm{Pseudo}}(\Omega) = \dot{\Phi}_{\mathrm{PseudoAnltc}}(\Omega) + \dot{\Phi}_{\mathrm{PseudoHiF}}(\Omega) \quad (16)$$

where $\dot{\Phi}_{\mathrm{PseudoAnltc}}(\Omega)$ is analytically definable pseudoconing and $\dot{\Phi}_{\mathrm{PseudoHiF}}(\Omega)$ is ill-defined generally high-frequency pseudoconing.

Based on the earlier discussion, the design requirement for the coning correction algorithm is to generate a $\delta\underline{\phi}_{\mathrm{Gyro}_l}$ value in Eq. (13) that will produce a $\Delta\underline{\Psi}_{\mathrm{Gyro}_l}$ solution using real gyro data whose summation buildup rate in attitude will equal the Eq. (11) true $\Delta\underline{\Psi}_{\mathrm{True}_l}$ summation buildup rate. From Eqs. (11) and (13) we see that the only terms generating an average summing attitude buildup rate are the leading $\underline{u}_c$ axis terms (as in [1–3,5,6]); the others generate cyclic bounded oscillations when summed. Thus, we specify that $\delta\underline{\phi}_{\mathrm{Gyro}_l}$ be set to equate the constant components of Eqs. (11) and (13). With rearrangement the result is

$$\delta\underline{\phi}_{\mathrm{Gyro}_l} = \underline{u}_c\left(\dot{\Phi}_{\mathrm{True}}(\Omega) - \dot{\Phi}_{\mathrm{Gyro}}(\Omega)\frac{\sin\Omega T_l}{\Omega T_l}\right)T_l \quad (17)$$

Equation (17) would be used as the design basis for coefficient determination in a frequency-based coning correction algorithm for the $\dot{\Phi}_{\mathrm{Gyro}}(\Omega)$ input expected in the user application. The resulting coefficients will then generate a true attitude solution in the presence of $\dot{\Phi}_{\mathrm{Gyro}}(\Omega)$ coning on gyro inputs (true plus pseudo) for that application.

For the real gyro data case addressed in [5], the coning rate content of the gyro output $\dot{\Phi}_{\mathrm{Gyro}}(\Omega)$ is $F(\Omega)^2\dot{\Phi}_{\mathrm{True}}(\Omega)$ where $F(\Omega)$ is the dynamic transfer function of a filter applied on the gyro input to the attitude updating algorithm (defined as the ratio of filtered to unfiltered amplitude responses to sinusoidal inputs at frequency Ω: see Appendix for example). Equations (15–17) show that this corresponds to

$$\dot{\Phi}_{\mathrm{PseudoAnltc}}(\Omega) = (F(\Omega)^2 - 1)\dot{\Phi}_{\mathrm{True}}(\Omega) \quad (18)$$

$$\delta\underline{\phi}_{\mathrm{Gyro}_l} = \dot{\Phi}_{\mathrm{True}}(\Omega)\left(1 - F(\Omega)^2\frac{\sin\Omega T_l}{\Omega T_l}\right)T_l \quad (19)$$

which agrees with the [5] result. This is significant because it also demonstrates the equality between the [5] solution based on constrained coning motion and Eq. (17) based on unconstrained coning. For the error-free gyro case addressed in [1–3,6], the coning rate content of the gyro output $\dot{\Phi}_{\mathrm{Gyro}}(\Omega)$ is $\dot{\Phi}_{\mathrm{True}}(\Omega)$. Substitution in Eq. (17) yields the [1–3,6] result

$$\delta\underline{\phi}_{\mathrm{Gyro}_l} = \dot{\Phi}_{\mathrm{True}}(\Omega)\left(1 - \frac{\sin\Omega T_l}{\Omega T_l}\right)T_l \quad (20)$$

Note also as in [2,3,6], that Eq. (20) is the analytic solution for $\delta\underline{\phi}_l$ in Eqs. (9) using Eq. (4) for angular rate $\underline{\omega}(t)$ and $\dot{\Phi}(\Omega)$ as defined in Eq. (8) for $\dot{\Phi}_{\mathrm{True}}(\Omega)$.

Designing Frequency-Based Coning Algorithm Coefficients

Frequency-based algorithms for the $\delta\underline{\phi}_l$ coning correction have had the general form [2,3,5,6]

$$\delta\underline{\phi}_{\mathrm{Algo}_l} = \left(\sum_{s=1}^{N-1} C_s\Delta\underline{\alpha}_{k-s}\right) \times \Delta\underline{\alpha}_k \quad \Delta\underline{\alpha}_k = \int_{t_{k-1}}^{t_k}\underline{\omega}dt \quad (21)$$

In an Eq. (14) coning environment it has been recognized ([2,3,5,6] and [7] Sec. 10.1.1.2.2) that the $\Delta\underline{\alpha}_{k-s} \times \Delta\underline{\alpha}_k$ terms in Eq. (21) are directed along $\underline{u}_c$ with magnitude $2\dot{\Phi}_{\mathrm{Gyro}}(\Omega)f_s(\beta)T_k$ where

$$f_s(\beta) = 2s\frac{\sin s\beta}{s\beta} - (s-1)\frac{\sin(s-1)\beta}{(s-1)\beta} - (s+1)\frac{\sin(s+1)\beta}{(s+1)\beta}$$
$$\beta \equiv \Omega T_k \quad (22)$$

with T_k the sensor sample time interval from t_{k-1} to t_k, and β a T_k normalized frequency parameter. Thus, $\delta\underline{\phi}_{\mathrm{Algo}_l}$ in Eq. (21) is equivalently

$$\delta\underline{\phi}_{\text{Algo}_l}(\Omega) = \underline{u}_c 2\dot{\Phi}_{\text{Gyro}}(\Omega) T_k \sum_{s=1}^{N-1} C_s f_s(\beta) \tag{23}$$

The desired output from the Eq. (21) coning correction algorithm is $\delta\underline{\phi}_{\text{Gyro}_l}$ from Eq. (17), or in normalized β frequency format

$$\delta\underline{\phi}_{\text{Gyro}_l} = \underline{u}_c \left(\dot{\Phi}_{\text{True}}(\Omega) - \dot{\Phi}_{\text{Gyro}}(\Omega) \frac{\sin(L_{kl}\beta)}{L_{kl}\beta} \right) L_{kl} T_k \tag{24}$$

where L_{kl} (the number of k cycles in an l cycle) is the ratio of k cycle sensor sampling to l cycle coning correction computation intervals ($L_{kl} = T_l/T_k$). We define the coning correction algorithm design error $e_{\text{Cone}_l}(\Omega)$ as the $\underline{u}_c$ component difference between the Eq. (23) algorithm output and the desired Eq. (24) response:

$$e_{\text{Cone}_l}(\Omega) = \left[2\dot{\Phi}_{\text{Gyro}}(\Omega) \sum_{s=1}^{N-1} C_s f_s(\beta) - \left(\dot{\Phi}_{\text{True}}(\Omega) - \dot{\Phi}_{\text{Gyro}}(\Omega) \frac{\sin(L_{kl}\beta)}{L_{kl}\beta} \right) L_{kl} \right] T_k \tag{25}$$

Minimizing $e_{\text{Cone}_l}(\Omega)$ in Eq. (25) has in effect been the design basis for previous frequency-based coning correction algorithms. The series expansion design method [1–3,5] expands Eq. (25) as a Taylor series in powers of normalized coning frequency and then sets the algorithm C_s elements to null the Taylor series expansion coefficients. The $e_{\text{Cone}_l}(\Omega)$ error in Eq. (25) is thereby equated to zero for the number of terms carried in the series. The series is truncated so that the number of terms carried matches the number of terms (and coefficients) used in the coning algorithm. The result is a set of null equations for the Taylor series coefficients that are solved simultaneously to determine the algorithm C_s coefficients. In [1–3], the Taylor series expansion process is simplified because $\dot{\Phi}_{\text{Gyro}}(\Omega)$ equals $\dot{\Phi}_{\text{True}}(\Omega)$, hence, both are eliminated from the expansion process upon setting Eq. (25) to zero. In [5], $\dot{\Phi}_{\text{Gyro}}(\Omega)$ is proportional to $\dot{\Phi}_{\text{True}}(\Omega)$, hence, the frequency-based proportionality factor $\dot{\Phi}_{\text{Gyro}}(\Omega)/\dot{\Phi}_{\text{True}}(\Omega)$ becomes part of the expansion process, adding analytical design complexity. Additionally, if high-frequency pseudoconing is included in the $\dot{\Phi}_{\text{Gyro}}(\Omega)$ definition, more terms may be required in the Taylor series expansion for accurate modeling. In contrast, the Explicit Frequency Shaping method for minimizing Eq. (25) [6] provides the advantage of not requiring analytical design for coefficient determination; only specifications for the $\dot{\Phi}_{\text{Gyro}}(\Omega)$ and $\dot{\Phi}_{\text{True}}(\Omega)$ profiles which are retained as a means for weighting $e_{\text{Cone}_l}(\Omega)$ in the minimization process.

Extended Explicit Coning Algorithm Coefficient Design

Following the Explicit Frequency Shaping design methodology in [6], the C_s coefficients are designed to minimize Eq. (25) in a least-squares integral sense over a user selected frequency range. The error to be minimized is z, the integral of $e_{\text{Cone}_l}(\Omega)$ squared over a user specified β frequency range β_{Range}:

$$z \equiv \int_{\beta=0}^{\beta=\beta_{\text{Range}}} [e_{\text{Cone}_l}(\Omega)]^2 \, \mathrm{d}\beta = \int_{\beta=0}^{\beta=\beta_{\text{Range}}} \left[2\dot{\Phi}_{\text{Gyro}}(\Omega) \sum_{s=1}^{N-1} C_s f_s(\beta) - \left(\dot{\Phi}_{\text{True}}(\Omega) - \dot{\Phi}_{\text{Gyro}}(\Omega) \frac{\sin(L_{kl}\beta)}{L_{kl}\beta} \right) L_{kl} \right]^2 T_k^2 \, \mathrm{d}\beta \tag{26}$$

Minimizing Eq. (26) takes the partial derivative with respect to each C_s and equates each to zero:

$$\int_{\beta=0}^{\beta=\beta_{\text{Range}}} \dot{\Phi}_{\text{Gyro}}(\Omega) f_r(\beta) \left[2\dot{\Phi}_{\text{Gyro}}(\Omega) \sum_{s=1}^{N-1} C_s f_s(\beta) - \left(\dot{\Phi}_{\text{True}}(\Omega) - \dot{\Phi}_{\text{Gyro}}(\Omega) \frac{\sin(L_{kl}\beta)}{L_{kl}\beta} \right) L_{kl} \right] \mathrm{d}\beta = 0$$

or

$$\sum_{s=1}^{N-1} C_s \left(\int_{\beta=0}^{\beta=\beta_{\text{Range}}} 2\dot{\Phi}_{\text{Gyro}}(\Omega)^2 f_r(\beta) f_s(\beta) \, \mathrm{d}\beta \right) = \int_{\beta=0}^{\beta=\beta_{\text{Range}}} \dot{\Phi}_{\text{Gyro}}(\Omega) f_r(\beta) \left(\dot{\Phi}_{\text{True}}(\Omega) - \dot{\Phi}_{\text{Gyro}}(\Omega) \frac{\sin(L_{kl}\beta)}{L_{kl}\beta} \right) L_{kl} \, \mathrm{d}\beta \tag{27}$$

Defining terms

$$a_{rs} \equiv \int_{\beta=0}^{\beta=\beta_{\text{Range}}} 2\dot{\Phi}_{\text{Gyro}}(\Omega)^2 f_r(\beta) f_s(\beta) \, \mathrm{d}\beta$$

$$b_r \equiv \int_{\beta=0}^{\beta=\beta_{\text{Range}}} \dot{\Phi}_{\text{Gyro}}(\Omega) f_r(\beta) \left(\dot{\Phi}_{\text{True}}(\Omega) - \dot{\Phi}_{\text{Gyro}}(\Omega) \frac{\sin(L_{kl}\beta)}{L_{kl}\beta} \right) L_{kl} \, \mathrm{d}\beta \tag{28}$$

then gives

$$A\underline{C}_s = \underline{b} \tag{29}$$

where A is an $N-1$ by $N-1$ square matrix formed from a_{rs} elements, $\underline{C}_s$ is a column matrix whose elements are the C_s coefficients, and $\underline{b}$ is a column matrix formed from the b_r elements. Rearrangement of Eq. (29) provides the C_s coefficients:

$$\underline{C}_s = A^{-1}\underline{b} \tag{30}$$

Equations (30) for $\underline{C}_s$ is then used in Eq. (21) to compute the coning correction term $\delta\underline{\phi}_{\text{Algo}_l}$. Equation (15) and (16) would be used for $\dot{\Phi}_{\text{Gyro}}(\Omega)$ in Eq. (28).

The previous development was based on Explicit coefficient optimization under specified discrete coning vs frequency conditions. As in [6], the technique can be extended to also cover stochastic angular rate environments in which coning might be present (e.g., coning generated by a linear random vibration source that induces correlated angular motion about two orthogonal angular rate sensor axes):

$$E(e_{\text{Cone}_l}) = \int_0^{\infty} \left[2\dot{\Phi}_{\text{GyroDens}}(\Omega) \left(\sum_{s=1}^{N-1} C_s f_s(\beta) \right) - \left(\dot{\Phi}_{\text{TrueDens}}(\Omega) - \dot{\Phi}_{\text{GyroDens}}(\Omega) \frac{\sin(L_{kl}\beta)}{L_{kl}\beta} \right) L_{kl} \right] \mathrm{d}\beta \tag{31}$$

where $E(\,)$ is the expected value operator and $\dot{\Phi}_{\text{TrueDens}}(\Omega)$, $\dot{\Phi}_{\text{GyroDens}}$ are density functions for true and gyro output coning of the sensor assembly such that the expected values of $\dot{\Phi}_{\text{True}}(\Omega)$ and $\dot{\Phi}_{\text{Gyro}}(\Omega)$ are given by

$$E(\dot{\Phi}_{\text{True}}) = \int_0^{\infty} \dot{\Phi}_{\text{TrueDens}}(\Omega) \, \mathrm{d}\Omega$$
$$E(\dot{\Phi}_{\text{Gyro}}) = \int_0^{\infty} \dot{\Phi}_{\text{GyroDens}}(\Omega) \, \mathrm{d}\Omega \tag{32}$$

Depending on the relative phasing of the correlated angular rate sensor responses between axes, $\dot{\Phi}_{\text{Dens}}(\Omega)$ will vary in magnitude and polarity as a function of Ω. The relative phasing is not easily predictable, making it difficult to evaluate Eq. (31) analytically. On a worst-case basis, Eq. (31) can be evaluated (as in [6]) by assuming phasing that maximizes $E(e_{\text{Cone}_l})$. Then Eq. (31) becomes

$$E(e_{\text{Cone}_l}) = \int_0^{\infty} \left| 2\frac{\dot{\Phi}_{\text{GyroDensMax}}(\Omega)}{T_k} \left(\sum_{s=1}^{N-1} C_s f_s(\beta) \right) - \left(\frac{\dot{\Phi}_{\text{TrueDensMax}}(\Omega)}{T_k} - \frac{\dot{\Phi}_{\text{GyroDensMax}}(\Omega)}{T_k} \frac{\sin(L_{kl}\beta)}{L_{kl}\beta} \right) L_{kl} \right| T_k \, \mathrm{d}\beta \tag{33}$$

An optimum set of C_s coefficients can be defined as those that minimize $E(e_{\text{Cone}_l})$ in Eq. (33). Because Eq. (33) is nonlinear in C_s,

there is no simple analytic method for evaluating the optimum coefficients, thereby requiring a numerical optimization method as a substitute. Alternatively (as in [6]), an analytically definable set of optimum coefficients can be generated as those that minimize the square of the Eq. (33) integrand over a design frequency range. Then the parameter to be minimized is z given by

$$z=\int_{\beta=0}^{\beta=\beta_{\text{Range}}}\left[2\frac{\dot{\Phi}_{\text{GyroDensMax}}(\Omega)}{T_k}\left(\sum_{s=1}^{N-1}C_s f_s(\beta)\right)-\left(\frac{\dot{\Phi}_{\text{TrueDensMax}}(\Omega)}{T_k}-\frac{\dot{\Phi}_{\text{GyroDensMax}}(\Omega)}{T_k}\frac{\sin(L_{kl}\beta)}{L_{kl}\beta}\right)L_{kl}\right]^2 T_k^2\,\mathrm{d}\beta \quad (34)$$

Comparing Eq. (34) with the Eq. (26) z expression minimized for optimum C_s under discrete inputs, we see that the minimization problems can be made equivalent by equating $\dot{\Phi}_{\text{TrueDens}}(\Omega)$ and $\dot{\Phi}_{\text{GyroDens}}$ in Eq. (26) to

$$\begin{aligned}\dot{\Phi}_{\text{True}}(\Omega)&=\dot{\Phi}_{\text{TrueDensMax}}(\Omega)/T_k\\ \dot{\Phi}_{\text{Gyro}}(\Omega)&=\dot{\Phi}_{\text{GyroDensMax}}(\Omega)/T_k\end{aligned} \quad (35)$$

With this substitution, the Eqs. (28) and (30) extended Explicit coefficient formulas can be used to optimize coefficients for a stochastic angular rate environment. The $\dot{\Phi}_{\text{GyroDensMax}}(\Omega)$ value for Eqs. (35) would be obtained analogous to Eq. (15) with (16):

$$\dot{\Phi}_{\text{GyroDensMax}}(\Omega)=\dot{\Phi}_{\text{TrueDensMax}}(\Omega)+\dot{\Phi}_{\text{PseudoDensMax}}(\Omega) \quad (36)$$

$$\dot{\Phi}_{\text{PseudoDensMax}}(\Omega)=\dot{\Phi}_{\text{PseudoDensMaxAnltc}}(\Omega)+\dot{\Phi}_{\text{PseudoDensMaxHiF}}(\Omega) \quad (37)$$

where $\dot{\Phi}_{\text{PseudoDensMaxAnltc}}(\Omega)$ is an analytically definable coning rate density and $\dot{\Phi}_{\text{PseudoDensMaxHiF}}(\Omega)$ is an ill-defined generally high-frequency pseudoconing density. For the filtered gyro data case addressed in [5], the analytically definable pseudoconing density would be computed similar to Eq. (18):

$$\dot{\Phi}_{\text{PseudoDensMaxAnltc}}(\Omega)=[F(\Omega)^2-1]\dot{\Phi}_{\text{TrueDensMax}}(\Omega) \quad (38)$$

For confirmation of acceptable results, algorithm coefficients derived with Eqs. (35–37) in Eq. (28) and (30) should be tested using the Eq. (33) worst-case formula. For this purpose, a more meaningful version of Eq. (33) is $E(\dot{e}_{\text{Cone}})$, the average expected error rate over an l cycle defined as $E(e_{\text{Cone}_l})$ divided by the l cycle time period T_l:

$$\begin{aligned}E(\dot{e}_{\text{Cone}})&\equiv E(e_{\text{Cone}_l})/T_l=E(e_{\text{Cone}_l})/(L_{kl}T_k)\\&=\int_0^{\infty}\left|\frac{2}{L_{kl}}\frac{\dot{\Phi}_{\text{GyroDensMax}}(\Omega)}{T_k}\left(\sum_{s=1}^{N-1}C_s f_s(\beta)\right)-\frac{\delta\dot{\phi}_{\text{GyroDensMax}}(\Omega)}{T_k}\right|\mathrm{d}\beta\end{aligned} \quad (39)$$

with

$$\delta\dot{\phi}_{\text{GyroDensMax}}(\Omega)\equiv\dot{\Phi}_{\text{TrueDensMax}}(\Omega)-\dot{\Phi}_{\text{GyroDensMax}}(\Omega)\frac{\sin(L_{kl}\beta)}{L_{kl}\beta} \quad (40)$$

where $\delta\dot{\phi}_{\text{GyroDensMax}}(\Omega)$ is a density function for the desired coning correction algorithm response in a random environment (based on the general formulation in [7] Sec. 10.4.1) for which $E(\delta\phi_{\text{Gyro}_l})$, the expected value equivalent to Eq. (17), would be

$$E(\delta\phi_{\text{Gyro}_l})=\int_0^{\infty}|\delta\dot{\phi}_{\text{GyroDensMax}}(\Omega)|T_l\,\mathrm{d}\Omega \quad (41)$$

For design purposes it is also useful to define the average desired algorithm response rate $E(\delta\dot{\phi}_{\text{Gyro}})$ as the l cycle Eq. (41) expected value $E(\delta\phi_{\text{Gyro}_l})$ divided by T_l:

$$E(\delta\dot{\phi}_{\text{Gyro}})\equiv E(\delta\phi_{\text{Gyro}_l})/T_l=\int_0^{\infty}\left|\frac{\delta\dot{\phi}_{\text{GyroDensMax}}(\Omega)}{T_k}\right|\mathrm{d}\beta \quad (42)$$

Evaluating Extended Explicit Coning Algorithm Performance

Extended Explicit coning correction algorithm performance was evaluated for the paper under discrete and stochastic coning conditions as described next.

Coning correction algorithm output rate in a discrete coning environment $\delta\dot{\phi}_{\text{Algo}}$ was evaluated as the average algorithm response to gyro inputs, calculated as the $\underline{u}_c$ component of the Eq. (23) coning correction l cycle algorithm $\delta\underline{\phi}_{\text{Algo}_l}(\Omega)$ divided by the l cycle time period T_l:

$$\begin{aligned}\delta\dot{\phi}_{\text{Algo}}(\Omega)&=2\dot{\Phi}_{\text{GyroEval}}(\Omega)T_k\left(\sum_{s=1}^{N-1}C_s f_s(\beta)\right)\Big/T_l\\&=\frac{2}{L_{kl}}\dot{\Phi}_{\text{GyroEval}}(\Omega)\left(\sum_{s=1}^{N-1}C_s f_s(\beta)\right)\end{aligned} \quad (43)$$

where $\dot{\Phi}_{\text{GyroEval}}(\Omega)$ is the gyro output coning rate used for performance evaluation (as contrasted with $\dot{\Phi}_{\text{Gyro}}(\Omega)$ used for Explicit algorithm coefficient design). The Eval notation in Eq. (43) allows for differences in coning rate values used for performance evaluation and coefficient determination. Similarly, $\dot{\Phi}_{\text{GyroEval}}(\Omega)$ was calculated as in Eqs. (15) and (16):

$$\dot{\Phi}_{\text{GyroEval}}(\Omega)=\dot{\Phi}_{\text{TrueEval}}(\Omega)+\dot{\Phi}_{\text{PseudoEval}}(\Omega) \quad (44)$$

$$\dot{\Phi}_{\text{PseudoEval}}(\Omega)=\dot{\Phi}_{\text{PseudoEvalAnltc}}(\Omega)+\dot{\Phi}_{\text{PseudoEvalHiF}}(\Omega) \quad (45)$$

Algorithm error for a discrete coning environment was evaluated as the average error buildup rate $\dot{e}_{\text{Cone}}(\Omega)$ defined as $e_{\text{Cone}_l}(\Omega)$ in Eq. (25) divided by T_l:

$$\begin{aligned}\dot{e}_{\text{Cone}}(\Omega)&=\frac{2}{L_{kl}}\dot{\Phi}_{\text{GyroEval}}(\Omega)\sum_{s=1}^{N-1}C_s f_s(\beta)\\&\quad-\left(\dot{\Phi}_{\text{TrueEval}}(\Omega)-\dot{\Phi}_{\text{GyroEval}}(\Omega)\frac{\sin(L_{kl}\beta)}{L_{kl}\beta}\right)\end{aligned} \quad (46)$$

For a stochastic coning environment, the expected algorithm error rate $E(\dot{e}_{\text{Cone}})$ was evaluated similarly based on Eqs. (39) and (40) with (36) and (37):

$$E(\dot{e}_{\text{Cone}})=\int_0^{\infty}\left|\frac{2}{L_{kl}}\frac{\dot{\Phi}_{\text{GyroDensMaxEval}}(\Omega)}{T_k}\left(\sum_{s=1}^{N-1}C_s f_s(\beta)\right)-\frac{\delta\dot{\phi}_{\text{GyroDensMaxEval}}(\Omega)}{T_k}\right|\mathrm{d}\beta \quad (47)$$

$$\delta\dot{\phi}_{\text{GyroDensMaxEval}}(\Omega)\equiv\dot{\Phi}_{\text{TrueDensMaxEval}}(\Omega)-\dot{\Phi}_{\text{GyroDensMaxEval}}(\Omega)\frac{\sin(L_{kl}\beta)}{L_{kl}\beta} \quad (48)$$

$$\dot{\Phi}_{\text{GyroDensMaxEval}}(\Omega)=\dot{\Phi}_{\text{TrueDensMaxEval}}(\Omega)+\dot{\Phi}_{\text{PseudoDensMaxEval}}(\Omega) \quad (49)$$

$$\dot{\Phi}_{\text{PseudoDensMaxEval}}(\Omega)=\dot{\Phi}_{\text{PseudoDensMaxEvalAnltc}}(\Omega)+\dot{\Phi}_{\text{PseudoDensMaxEvalHiF}}(\Omega) \quad (50)$$

Numerical Examples: Algorithm Coefficient Design

To illustrate the characteristics of the Extended Explicit compared with original Explicit and Frequency-series designed coning correction algorithms, seven algorithm configurations were evaluated, each (as in [6]) having $N = 4$ (four sequential $\Delta\underline{\alpha}$ samples in the $\delta\underline{\phi}_{\text{Algo}_l}$ calculation), $L_{kl} = N$ (coning correction computation l cycle rate N times slower than the sensor sample k rate such that all $\Delta\underline{\alpha}$ samples for $\delta\underline{\phi}_{\text{Algo}_l}$ determination are contained within the current l cycle), and $T_k = 0.001$ s (1 KHz gyro sampling rate):

1) EXplDscrt-Extended Explicit (EXpl) with coefficients designed for gyro output filtering in discrete (Dscrt) coning environments.

2) EXplRnd-Extended Explicit (EXpl) with coefficients designed for gyro output filtering in random (Rnd) coning environments.

3) EXplRndwCtf-Extended Explicit (EXpl) with coefficients designed for gyro output filtering and high-frequency pseudoconing response cutoff (wCtf) in random (Rnd) coning environments.

4) Mk/TzFSr-Mark/Tazartes frequency series with coefficients designed as in [5].

5) TrdXplDscrt-Traditional Explicit (TrdXpl) with coefficients designed for true gyro inputs without pseudoconing in discrete (Dscrt) coning environments (as in [6]).

6) TrdFSr-Traditional frequency-series with coefficients designed for true gyro inputs without pseudoconing (as in [1–3]).

7) Bas-Baseline (Bas) reference configuration with zero for coning correction coefficients.

Extended Explicit algorithm designed coefficients were based on having a [5]-type moving average filter (see Appendix) on the gyro data input to the algorithm with transfer function

$$F(\Omega) = \sin(\Omega T_k/2)/(\Omega T_k/2) \tag{51}$$

and analytically definable pseudoconing in Eqs. (16) and (37) set as in Eq. (18) to

$$\dot{\Phi}_{\text{PseudoAnltc}}(\Omega) = [F(\Omega)^2 - 1]\dot{\Phi}_{\text{True}}(\Omega)$$
$$\dot{\Phi}_{\text{PseudoDensMaxAnltc}}(\Omega) = [F(\Omega)^2 - 1]\dot{\Phi}_{\text{TrueDensMax}}(\Omega) \tag{52}$$

The Mk/TzFSr coefficients were taken from [5] as calculated for the Eq. (51) gyro data filter.

For the Explicit discrete environment designed coefficients (EXplDscrt and TrdXplDscrt) using Eqs. (15) and (16) in Eqs. (28) and (30), $\dot{\Phi}_{\text{True}}(\Omega)$ was set to unity for β/π from 0 to 0.2, and zero for β/π greater than 0.2, thereby approximating the true coning region expected for a vibration isolated sensor assembly with imbalance and a 50 Hz $= 100\pi$ rad/s linear resonance frequency (i.e., $\beta/\pi = 0.1$ for $T_k = 0.001$ s). (Note: [6] describes how a $\dot{\Phi}_{\text{True}}(\Omega)$ analytical model can be easily constructed for a sensor assembly that includes isolator imbalance resonance and maneuver induced coning effects.) Additionally, β_{Range} was set to π and $\dot{\Phi}_{\text{PseudoHiF}}(\Omega)$ was set to zero.

For the Explicit random environment designed coefficients using Eqs. (35–37) in (28) and (30), $\dot{\Phi}_{\text{TrueDensMax}}(\Omega)/T_k$ was as shown in Fig. 1 (taken from [6]) representing the coning spectrum for a vibration isolated sensor assembly with a 50 Hz linear resonance frequency and 2% isolator imbalance under a 7.6 g root-mean-square (rms) broadband random vibration exposure (3.6 gs rms into the gyros). Corresponding to the selected $\dot{\Phi}_{\text{TrueDensMax}}(\Omega)/T_k$ profile, Fig. 1 includes a plot of $|\delta\dot{\phi}_{\text{GyroDensMax}}(\Omega)/T_k|$ calculated using Eqs. (40), (36), (37), (51), and (52) for $\dot{\Phi}_{\text{PseudoDensMaxHiF}}(\Omega)$ in Eq. (37) set to zero. The associated desired expected coning correction algorithm rate $E(\delta\dot{\phi}_{\text{Gyro}})$ is 0.4138 deg/h, the integral of $|\delta\dot{\phi}_{\text{GyroDensMax}}(\Omega)/T_k|$ in Fig. 1 as indicated from Eq. (42).

The EXplRnd coefficients (designed for random environments) are based on zero for high-frequency pseudoconing $\dot{\Phi}_{\text{PseudoDensMaxHiF}}(\Omega)$. In contrast, the EXplRndwCtf random environment coefficients are designed for the presence of a hypothetical high-frequency pseudoconing component as a means for attenuating high-frequency response to potential pseudoconing

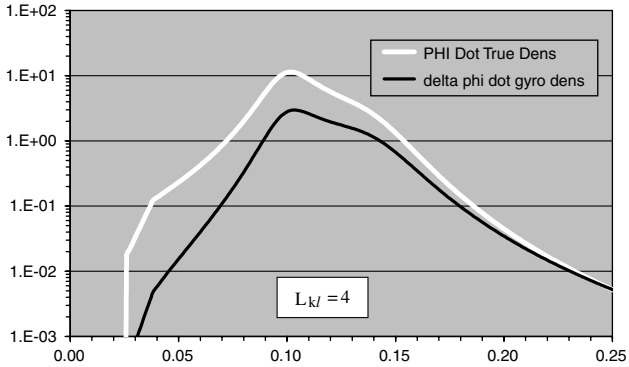

Fig. 1 $\dot{\Phi}_{\text{TrueDensMax}}(\Omega)/T_k$ **and** $\delta\dot{\phi}_{\text{GyroDensMax}}(\Omega)/T_k$ **in [(deg/h)/(rad/s)]/s vs** β/π**.**

error (a conservative design practice). As such, $\dot{\Phi}_{\text{PseudoDensMaxHiF}}(\Omega)$ was represented as constant for frequencies higher than a specified start-up frequency $\beta/\pi = 0.335$ pirads (i.e., 168 Hz), the frequency in Fig. 1 where integrated $|\delta\dot{\phi}_{\text{GyroDensMax}}(\Omega)/T_k|$ (i.e., a portion of $E(\delta\dot{\phi}_{\text{Gyro}})$ using Eq. (42)) was within 0.0002 deg/h of the fully integrated 0.4138 deg/h value. This corresponds to 2% of the 0.01 deg/h gyro accuracy requirement in a typical aircraft INS, a conservative design specification for the coning algorithm error. Similarly, the magnitude of $\dot{\Phi}_{\text{PseudoDensMaxHiF}}(\Omega)$ was set to 0.00221[(deg/h)/(rad/s)]/s to limit the Eq. (39) expected error $E(\dot{e}_{\text{Cone}})$ to less than 0.0002 deg/h.

Coefficients for the seven coning correction algorithms are presented in Table 1.

Numerical Examples: Coefficient Performance Evaluation

All performance data obtained were calculated for filtered gyro inputs using the same evaluation equations and associated evaluation software program. The only factor distinguishing one algorithm's performance from another was the numerical value of their Table 1 coefficients (although they were determined using different design methodologies). Thus, the performance data presented in this paper (and in [6]) can also be interpreted as a simple comparison between performance obtained using different numerical values for coning coefficients, regardless of how they were generated.

For Table 1 algorithm coefficient performance evaluation in discrete environments, algorithm response $\delta\dot{\phi}_{\text{Algo}}(\Omega)$ was calculated using Eq. (43) with $\dot{\Phi}_{\text{GyroEval}}(\Omega)$ set to unity (normalized) over all frequencies; algorithm error $\dot{e}_{\text{Cone}}(\Omega)$ was calculated using Eq. (46) with $\dot{\Phi}_{\text{TrueEval}}(\Omega)$ set to unity (normalized) and analytical pseudoconing error $\dot{\Phi}_{\text{PseudoAnltc}}(\Omega)$ set as specified in Eq. (52) with Eq. (51) (i.e., the value used for EXplDscrt and Mk/TzFSr Table 1 coefficient design). Expected algorithm error in a random environment $E(\dot{e}_{\text{Cone}})$ was calculated for the Table 1 coefficients using Eqs. (47) with $\dot{\Phi}_{\text{GyroDensMaxEval}}(\Omega)/T_k$ and $\delta\dot{\phi}_{\text{GyroDensMaxEval}}(\Omega)/T_k$ from Fig. 1 (which includes Eq. (52) with (51) for $\dot{\Phi}_{\text{PseudoDensMaxEvalAnltc}}(\Omega)$, the design basis for the EXplRnd and EXplRndwCtf Table 1 coefficients). For all discrete and random

Table 1 Coning correction algorithm coefficients ($N = 4, L_{kl} = 4$)

Coning algorithm	C1	C2	C3
EXplDscrt	2.39137	0.75633	0.53201
EXplRnd	2.39126	0.75646	0.53196
EXplRndwCtf	1.37429	1.58186	0.32110
Mk/TzFSr	2.36892	0.77487	0.52712
TrdXplDscrt	2.04932	0.86692	0.51673
TrdFSr	2.03810	0.87619	0.51429
Bas	0	0	0

environment performance evaluations, high-frequency pseudoconing components $\dot{\Phi}_{\text{PseudoEvalHiF}}$ and $\dot{\Phi}_{\text{PseudoDensMaxEvalHiF}}(\Omega)$ were set to zero.

Expected algorithm error results for the seven coning correction algorithms in random coning environments are presented in Table 2. Figures 2 and 3 present absolute value plots of resulting algorithm normalized response $\delta\dot{\phi}_{\text{Algo}}(\Omega)$ and error $\dot{e}_{\text{Cone}}(\Omega)$ for discrete coning environments. Note in Fig. 2 that the response curves for EXplDscrt, EXplRnd and Mk/TzFSr essentially overlap as do the TrdXplDscrt and TrdFSr curves in Figs. 2 and 3.

Comparing algorithm errors under random environments, Table 2 shows that for coefficients designed without high-frequency pseudoconing provisions, Extended Explicit algorithm performance (EXplDscrt and EXplRnd) is superior to the others tested. Adding high-frequency pseudoconing provisions to attenuate high-frequency gain (EXplRndwCtf) increases algorithm error, but within the 0.0002 deg/hr design limit established for pseudoconing amplitude selection (the basis for the coefficient design as discussed previously). The associated impact on algorithm response performance is evident in Fig. 2, demonstrating how the Explicit technique shapes the algorithm response to curtail the likelihood of high-frequency pseudoconing error buildup in the attitude computation (EXplRndwCtf). A corresponding sacrifice in discrete coning accuracy is also apparent in Fig. 3. When high-frequency pseudoconing is not of concern, Fig. 3 illustrates the balanced accuracy vs frequency characteristic of the Extended Explicit compared with the equivalent Mark/Tazartes Frequency-series algorithm (EXplDscrt or EXplRnd vs Mk/TzFSr) over the frequency range for expected true coning (β/π from 0 to 0.2). The Mk/TzFSr algorithm sacrifices midfrequency performance for high accuracy at lower frequencies. In contrast, the Extended Explicit algorithms achieve balanced

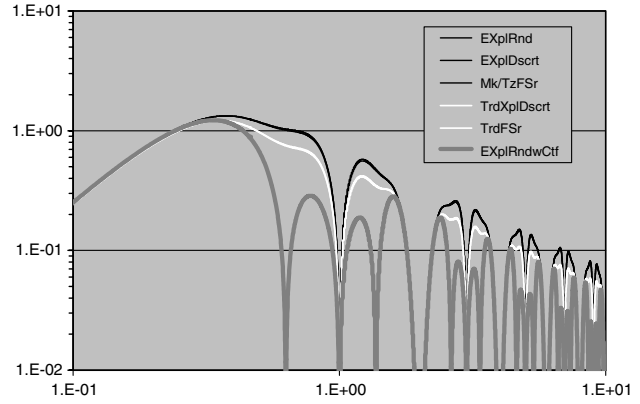

Fig. 2 Coning correction algorithm normalized response ($N = 4$, $L_{kl} = 4$): $\delta\dot{\phi}_{\text{Algo}}(\Omega)$ deg/h algorithm output per $\dot{\Phi}_{\text{GyroEval}}(\Omega)$ deg/h input vs β/π.

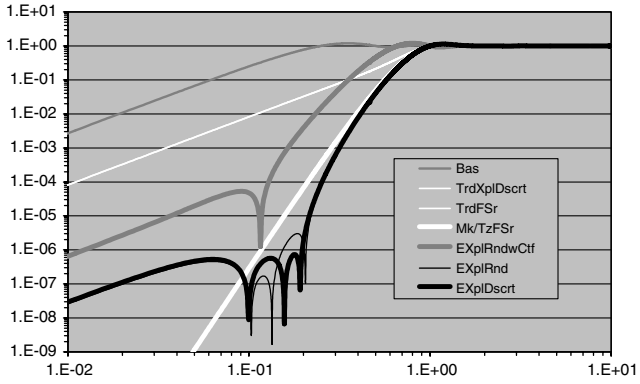

Fig. 3 Coning correction algorithm discrete normalized error ($N = 4$, $L_{kl} = 4$): $\dot{e}_{\text{Cone}}(\Omega)$ deg/h error per $\dot{\Phi}_{\text{TrueEval}}(\Omega)$ deg/h true coning vs β/π.

Table 2 Coning correction algorithm errors in random environment ($N = 4$, $L_{kl} = 4$)

Coning correction algorithm	Error (deg/h)
EXplDscrt	3.5801E − 6
EXplRnd	3.4543E − 6
EXplRndwCtf	1.9893E − 4
Mk/TzFSr	6.3140E − 6
TrdXplDscrt	1.4118E − 2
TrdFSr	1.4120E − 2
Bas	0.4138E0

performance across the low to midfrequency range. All algorithms investigated exhibited significant performance advantages in Table 2 and Fig. 3 compared with the Bas configuration which ignores coning correction completely (i.e., equating $\underline{\phi}_l$ to $\underline{\alpha}_l$ in Eq. (3)).

As expected, the traditional Explicit discrete and frequency-series algorithms (TrdXplDscrt and TrdFSr) have the poorest performance in Table 2 and Fig. 3 because they were not designed for operation with filtered gyro inputs (as were the other algorithms), and all performance figures in Table 2 and Fig. 3 are based on using Eq. (51) gyro data filtering. Interestingly, the Fig. 2 algorithm response characteristic for the TrdXplDscrt and TrdFSr algorithms have superior high-frequency pseudoconing attenuation characteristics compared with the other algorithms, the exception being the EXplRndwCtf algorithm which was explicitly designed for high-frequency pseudoconing attenuation. It is also to be noted that if performance evaluation was based on using unfiltered gyro data, the converse of the Table 2 and Fig. 3 results would be obtained, i.e., TrdXplDscrt and TrdFSr would have significantly better accuracy compared with the EXpl and MkFSr algorithms optimized for filtered inputs. The lesson is that the algorithm design should be selected to match the gyro input configuration for the intended application.

Performance Comparison with References

Performance comparisons between results presented in this and other referenced papers (particularly [5,6]) are not easily made because of differences in evaluation methods used and, for the Explicit algorithms, differences in their design criteria. Explicit performance data in [6] is based on error-free gyro inputs; in contrast this paper is based on filtered gyro inputs. Coefficients for Explicit Discrete algorithms in the [6] design were based on a hypothetical true coning environment for expected maneuver environments with isolator amplification/attenuation; a uniform-with-cutoff profile was used in this paper. The [5] performance equivalents to Figs. 2 and 3 are difficult to compare because [5] results are based on relative normalization (i.e., divided by the desired algorithm response function [Eq. (17) herein], using the true or filtered value for $\dot{\Phi}_{\text{Gyro}}(\Omega)$, depending on whether the algorithm being evaluated was designed for filtered or unfiltered inputs. One comparison that can safely be made is between the EXplRnd random environment error of 3.45E − 6 deg/h in Table 2 compared with the equivalent 2.55E − 6 deg/h error for XplRnd in Table 2 of [6]. The increased error for Table 2 herein is directly attributable to introducing the moving average filter, the only difference in the two configurations. This illustrates that adding a filter on gyro input data generally degrades dynamic performance, hence, should be avoided unless necessary for other reasons (e.g., to reduce quantization noise as discussed in [5,10]). Note also, that use of a gyro filter adds an undesirable dynamic lag to attitude algorithm outputs (half the averaging time for the moving average filter analyzed in this paper: see Eq. (A2) of the appendix).

The concept of adding high-frequency pseudoconing attenuation to the coning correction algorithm (as in the EXplRndwCtf configuration) is a generally desirable property as noted in [5], providing that it has negligible impact on true coning computational accuracy. This is easily achieved with the Extended Explicit technique by applying the same method used for the EXplRndwCtf design, but

without the analytic filter in the coefficient design (unless it is used on the actual gyro data). The filter was included in this paper to illustrate how the Extended Explicit technique can be used to optimize performance when operating with analytically definable pseudoconing and, for performance evaluation, to generate Explicit coefficients that are directly comparable to those of [5] designed using frequency-series expansion for the same analytic pseudoconing configuration.

Conclusions

The extended Explicit Frequency Shaping method for coning algorithm design is general, allowing coefficient optimization for gyro inputs that may or not contain pseudoconing. For coefficient determination, true and pseudoconing can be defined analytically or numerically. The extended Explicit technique can be used to compensate predictable pseudoconing error or, as a conservative design practice, to create a high-frequency cutoff in the coning algorithm response to attenuate potential pseudoconing effects that may exist outside the expected true coning region. Comparisons against previous frequency-series-based coning correction algorithms show improved accuracy in discrete or random coning environments.

Appendix: Moving Average Filter

A moving average filter calculates the average of the sequence of current plus $M-1$ past input values (M in total) at each filter output sampling cycle. As the sampling time moves forward in time, the averaging window moves forward to keep the average current. The filter output y_i at sample time i is analytically defined by

$$y_i = \frac{1}{M}\sum_{j=1}^{M} x_{i+1-j} \tag{A1}$$

where x_i is the filter input at sample time i and M is the averaging size (window). Reference [10] describes the moving average filter used on gyro data in [5] to reduce quantization noise. The x_i input to the filter represents an integrated gyro sensed angular rate increment over a small time interval δt, the time between filter cycles (e.g., one thousandth of the k cycle time period associated with Eq. (21) $\Delta\underline{\alpha}_k$ sampling). Thus, y_i represents the integrated input rate divided by M. The $\Delta\underline{\alpha}_k$ integrated rate increment in Eq. (21) is then calculated by summing M sequential y_is over a k cycle (as described in [10]). The response of the filter to a unity amplitude sinusoidal angular rate input is derived as the integrated angular rate over the filter time window divided by M. For M set to correspond to the width of one k cycle T_k (as in [10]), the result is

$$\begin{aligned} y_i &= \frac{1}{M}\int_{t_i-T_k}^{t_i} \sin\Omega\tau\,\mathrm{d}\tau = -\frac{1}{\Omega M}\cos\Omega\tau\Big]_{t_i-T_k}^{t_i} \\ &= -\frac{1}{\Omega M}[\cos\Omega t_i - \cos\Omega(t_i - T_k)] \\ &= \frac{2}{\Omega M}\sin\frac{\Omega T_k}{2}\sin\Omega\left(t_i - \frac{T_k}{2}\right) \end{aligned} \tag{A2}$$

The i cycle x_i input to the Eq. (A1) filter is the integrated sinusoidal input over an i cycle [derived analogously to Eq. (A2)]:

$$x_i = \int_{t_i-\delta t}^{t_i} \sin\Omega\tau\,\mathrm{d}\tau = \frac{2}{\Omega}\sin\frac{\Omega\delta t}{2}\sin\Omega\left(t_i - \frac{\delta t}{2}\right) \tag{A3}$$

The filter transfer function $F(\Omega)$ is defined as the ratio of the Eq. (A3) y_i output amplitude to the Eq. (A2) x_i input amplitude which, for $\delta t = T_k/M$, is

$$\begin{aligned} F(\Omega) &= \left(\sin\frac{\Omega T_k}{2}\right)\Big/\left(M\sin\frac{\Omega\delta t}{2}\right) \\ &= \left(\sin\frac{\Omega T_k}{2}\right)\Big/\left(M\sin\frac{\Omega T_k}{2M}\right) \end{aligned} \tag{A4}$$

For ΩT_k small compared with $2M$, Eq. (A4) approximates to the [5] and Eq. (51) form:

$$F(\Omega) \approx \left(\sin\frac{\Omega T_k}{2}\right)\Big/\left(\frac{\Omega T_k}{2}\right) \tag{A5}$$

A recursive computational algorithm for y_i is the differential form of Eq. (A1) (as illustrated in [10]):

$$\begin{aligned} y_i &= \frac{1}{M}\sum_{j=1}^{M} x_{i+1-j} = \frac{1}{M}\left(x_i + \sum_{j=1}^{M} x_{i-j} - x_{i-M}\right) \\ &= y_{i-1} + \frac{1}{M}(x_i - x_{i-M}) \end{aligned} \tag{A6}$$

Direct implementation of Eq. (A6) can impose a formidable throughput problem, depending on the manner used for generating the x_{i-M} past value term. In general, x_{i-M} is obtained as the last entry in a sequential reverse time file x_s of M saved past x_i values. A brute-force approach would update the x_s file at each filter cycle by, beginning at element $j = M$, sequentially setting in reverse order $x_s(j)$ to $x_s(j-1)$, and ending with $x_s(1)$ set to the current i cycle sampled x_i (i.e., M operations per filter i cycle).

An alternative method that imposes significantly less throughput is based on recognition that for each i cycle only two locations in the x_s file are impacted with new data each i cycle; $x_s(1)$ which is set to the latest x_i value, and $x_s(M)$ which is discarded in the updating process. The remaining x_s elements are shifted into the adjacent locations, intact at their previous values. The equivalent can be implemented for less throughput but more memory using an x_s file containing all past x_i values. The file would be structured in forward time so that the x_s element for the current x_i entry is one increment higher than for the previous entry. The result would require a file as long as the total number of filter cycles expected over the application time. Another approach requiring less throughput and less memory employs a reverse time circular buffer x_{cb} file of length M for x_s (as in [10]).

With an M element circular buffer, the file is treated as forming an imaginary circle having an M element circumference such that element M becomes adjacent to element 1 (analogous to the 360 deg point on a closed circular arc relative to the 1 deg point). The point on the circle M elements delayed from the current x_i entry is located for retrieval by a pointer index p that is decremented by one each filter cycle, thereby traversing the circle by one element each filter cycle in the direction of descending elements. When the pointer reaches element 0 it is reset to M, indicating that a full circle has been traversed (similar to identifying the 0 deg point on a closed circular arc as the equivalent to 360). After using the pointer to retrieve the M delayed x_i element from x_{cb}, the current x_i input is entered M increments delayed from the current pointer location in x_{cb} which, because of file circularity, corresponds to placement in the x_{cb} location currently specified by the pointer. When the pointer is decremented for the next filter cycle, the previously placed x_i location will then be $M-1$ cycles delayed in the x_{cb} file from the new pointer designation, to be retrieved M cycles later. The overall concept is illustrated next as pseudocode:

$p = p - 1$! Updates x_{cb} circular buffer element M pointer index p to maintain correspondence with M locations removed from the current filter i cycle.

If (p. EQ. 0) $p = M$! Controls x_{cb} buffer circularity by identifying the virtual element 0 location as being M cycles distant from element 1 in the M element x_{cb} circular file.

$y_i = y_{i-1} + [x_i - x_{\mathrm{cb}}(p)]/M$! calculates the current moving average filter i cycle output.

$x_{\mathrm{cb}}(p) = x_i$! inserts the current x_i value into the x_{cb} file location currently designated by pointer index p for retrieval M cycles later for y_i computation.

Repeat the above for each moving average filter i cycle.

The previous pseudocode represents the totality of computations that would be required for the moving average filter each filter output sample cycle.

Acknowledgment

In an earlier version of this paper, the extended Explicit coning correction algorithm design was based on generating a true value for the integrated coning portion of the rotation vector rate equation in the presence of pseudoconing on input gyro data. The fallacy in this approach noted in the current paper was uncovered and corrected during the review process thanks to questions raised by one of the reviewers.

References

[1] Miller, R., "A New Strapdown Attitude Algorithm," *Journal of Guidance, Control, and Dynamics*, Vol. 6, No. 4, July–Aug. 1983, pp. 287–291.
doi:10.2514/3.19831

[2] Ignagni, M. B., "Optimal Strapdown Attitude Integration Algorithms," *Journal of Guidance, Control, and Dynamics*, Vol. 13, No. 2, March–April 1990, pp. 363–369.
doi:10.2514/3.20558

[3] Ignagni, M. B., "Efficient Class of Optimized Coning Compensation Algorithms," *Journal of Guidance, Control, and Dynamics*, Vol. 19, No. 2, March–April 1996, pp. 424–429.
doi:10.2514/3.21635

[4] Laning, J. H., Jr., "The Vector Analysis of Finite Rotations and Angles," Massachusetts Inst. of Technology Instrumentation Lab. Special Rept. 6398-S-3, Cambridge, MA, 1949.

[5] Mark, J. G., and Tazartes, D. A., "Tuning of Coning Algorithms to Gyro Data Frequency Response Characteristics," *Journal of Guidance, Control, and Dynamics*, Vol. 24, No. 4, July–Aug. 2001, pp. 641–647.
doi:10.2514/2.4770

[6] Savage, P. G., "Coning Algorithm Design by Explicit Frequency Shaping," *Journal of Guidance, Control, and Dynamics*, Vol. 33, No. 4, July–Aug. 2010, pp. 1123–1132.
doi:10.2514/1.47337

[7] Savage, P. G., *Strapdown Analytics*, 2nd ed., Strapdown Associates, Maple Plain, MN, 2007.

[8] Savage, P. G., "Strapdown System Algorithms," *Advances in Strapdown Inertial Systems*, NATO AGARD Lecture Series No. 133, May 1984, Section 3.

[9] Savage, P. G., "Advances in Strapdown Sensors," *Advances in Strapdown Inertial Systems*, NATO AGARD Lecture Series No. 133, May 1984, Section 2.

[10] Mark, J. G., and Tazartes, D. A., "Resolution Enhancement Technique for Laser Gyroscopes," *Proceedings of the Fourth International Conference on Integrated Navigation Systems*, St. Petersburg, Russia, 1997, pp. 378–387.